Vectorial complex ray model and application to two-dimensional scattering of plane wave by a spheroidal particle

Kuan Fang Ren,[1,*] Fabrice Onofri,[2] Claude Rozé,[1] and Thierry Girasole[1]

[1]*UMR 6614/CORIA, CNRS—Université and INSA de Rouen Avenue de l'Université BP 12, 76801 St-Etienne du Rouvray, France*

[2]*UMR 6595/IUSTI, CNRS and Université d'Aix-Marseille, Technopôle Château Gombert, 13453 Marseille, France*

**Corresponding author: fang.ren@coria.fr*

Received October 27, 2010; revised December 6, 2010; accepted December 10, 2010;
posted December 20, 2010 (Doc. ID 137251); published January 27, 2011

A vectorial complex ray model is introduced to describe the scattering of a smooth surface object of arbitrary shape. In this model, all waves are considered as vectorial complex rays of four parameters: amplitude, phase, direction of propagation, and polarization. The ray direction and the wave divergence/convergence after each interaction of the wave with a dioptric surface as well as the phase shifts of each ray are determined by the vector Snell law and the wavefront equation according to the curvatures of the surfaces. The total scattered field is the superposition of the complex amplitude of all orders of the rays emergent from the object. Thanks to the simple representation of the wave, this model is very suitable for the description of the interaction of an arbitrary wave with an object of smooth surface and complex shape. The application of the model to two-dimensional scattering of a plane wave by a spheroid particle is presented as a demonstration.

OCIS codes: 080.0080, 290.5850, 260.3160, 080.1753, 290.5825.

Geometrical optics is a very simple and intuitive method for treating the interaction of an object with light or electromagnetic waves when a dimension of the object is much larger than the wavelength [1,2]. One of its main advantages over other methods is that it can be applied to objects of complex shape, which are hard or even impossible to be dealt with by rigorous theories or most numerical techniques. The variable separation methods based on the solution of Maxwell equations (or its equivalents) are limited to objects that can be described in a coordinate system of the same geometry, such as sphere, spheroid, ellipsoid, or circular or elliptical cylinder. Even in these "simple" cases, the numerical calculation remains another obstacle. Except for the sphere and the circular cylinder, the size of the scatterer can hardly exceed a few tens of wavelengths. Numerical methods such as T matrix, discrete multipole approximation, etc., can be applied to nonspherical particles, but the size parameter of the scatter is also severely limited [3].

Many researchers have contributed to the improvement of geometrical optics. Some take into account the forward diffraction or other particular wave effects (Airy theory for the rainbow [4] and Marston's model for the critical scattering [5]). Others combine directly geometrical optics with the electromagnetic wave method [6]. However, in these studies interference effects of all order rays are rarely taken into account. We have shown that, by taking into account the interferences between all scattered rays, as well as forward diffraction, we can predict correctly the scattering diagram in all directions [7,8], although the scattering diagram near the critical and rainbow angles is still to be improved. But, as soon as geometrical optics is extended to a three-dimensional (3D) object of irregular shape, three difficulties are encountered: (1) determination of reflection and refraction angles; (2) calculation of local divergence factors for smooth dielectric surfaces; and (3) phase shift due to focal lines. To overcome these obstacles, we are developing a so-called vectorial complex rays model (VCRM) that consists of three points: the rays are dealt with by vectors; the divergence and the focal line phase shifts are calculated by differential geometry; and the total scattered field is the superposition of the contributions of all complex rays. This model makes it possible to calculate the divergence factor of a single ray bundle and is easy to extend to irregularly shaped 3D objects. In this Letter, we present the general forms of VCRM for an irregularly shaped 3D object with examples of numerical results for the scattering of a plane wave by a spheroid at oblique incidence.

In a VCRM, the wave is considered as bundles of vectorial complex rays. Each ray, q, is characterized by four parameters: amplitude, $A_{q\mu}$, phase, Φ_q, direction of propagation, $\hat{k}_q$, and polarization state, μ:

$$\mathbf{S}_{q\mu} = A_{q\mu} e^{i\Phi_q} \hat{\mathbf{k}}_q, \tag{1}$$

where $\mu = 1, 2$ stands for perpendicular and parallel polarizations, respectively. The direction of the rays before and after reflection or refraction are described respectively by the normalized wave vectors $\hat{\mathbf{k}}_q = \mathbf{k}_q/k$ and $\hat{\mathbf{k}}'_q = \mathbf{k}'_q/k'$, and the two wave vectors $\mathbf{k}_q$ and $\mathbf{k}'_q$ are related by the vector Snell law:

$$(\mathbf{k}'_q - \mathbf{k}_q) \times \hat{\mathbf{n}} = 0, \tag{2}$$

where $\hat{\mathbf{n}}$ is the normal of the dioptric surface.

The amplitude of the ray is determined by the Fresnel coefficient, $\epsilon_{q\mu}$, and the divergence coefficient, D_q:

$$A_{q\mu} = \sqrt{D_q} |\epsilon_{q\mu}|. \tag{3}$$

The divergence coefficient, D_q, of an emergent ray after q time interactions with the dioptric surface is determined by curvature radii of the wavefronts according to

$$D_q = \frac{R'_{11}R'_{21}}{R_{12}R_{22}} \cdot \frac{R'_{12}R'_{22}}{R_{13}R_{23}} \cdots \frac{R'_{1q}R'_{2q}}{(r+R'_{1q})(r+R'_{2q})}, \tag{4}$$

where r is the distance between the emergent point to the observation point, R_{1j} and R_{2j} $(j = 1, 2, \ldots, q)$ are the two principal radii of curvature of the incident wave, and R'_{1j} and R'_{2j} $(j = 1, 2, \ldots, q)$ are those of the refracted wave. In fact, $1/(R_{1j}R_{2j})$ and $1/(R'_{1j}R'_{2j})$ are respectively the Gauss curvatures of the incident and the refracted wavefronts, and they can be determined by the curvature matrix of the corresponding surface [9].

Suppose that an arbitrary wave of curvature matrix Q impinges on a dioptric surface of curvature matrix C. Then, based on the procedure proposed by Deschamps [9], we deduce that the curvature matrix Q' of the wave after refraction is given by the wavefront matrix equation

$$(\mathbf{k}' - \mathbf{k}) \cdot \hat{\mathbf{n}} C = k'\Theta'^T Q' \Theta' - k\Theta^T Q \Theta, \tag{5}$$

where the letters with primes represent the quantities after refraction, T the transpose of the matrix, and Θ the projection matrix between the unitary vectors of the coordinates systems on the planes tangent to the wavefront and the dioptric surface.

The phase of an emergent ray is composed of four parts: (1) the phase of the incident wave, Φ_{inc}; (2) the phase due to the optical path, Φ_{path}, which can be computed directly according to the optical trajectory; (3) the phase due to the focal point or focal line, Φ_{focal} (each time the sign of the curvature radius, R_{ij}, changes we add a phase shift, $\pi/2$ [1]); and (4) the phase due to the reflection, $\Phi_{\lambda/2}$ (an additional phase, π, is added when the Fresnel coefficient is negative). The total phase of a ray is then

$$\Phi = \Phi_{\text{inc}} + \Phi_{\text{path}} + \Phi_{\text{focal}} + (\Phi_{\lambda/2}). \tag{6}$$

Knowing the amplitude and the phase of each ray, we calculate the total scattered field by the superposition of the complex amplitude of all orders of the rays emergent from the object.

It should be pointed out that the equations given above [Eqs. (2)–(6)] are valid for both the refraction and the reflection, and in the latter case we take $\mathbf{k}' \cdot \hat{\mathbf{n}} = -\mathbf{k} \cdot \hat{\mathbf{n}}$.

To validate this model, we have shown theoretically that in the special case of scattering of a plane wave by a sphere and an infinite circular cylinder at normal incidence, the forms of VCRM leads to the classical formulation as given, for example, by [1,4]. Numerical validation for a spherical bubble in water and a spheroid will be given later in the Letter.

As a demonstration, we apply the model presented above to the scattering of a spheroid particle illuminated by a plane wave. We are interested in the scattering in the plane defined by the symmetric axis of the particle and the direction of the incident wave, so this is a two-dimensional (2D) problem.

Consider a spheroid with the center at the origin of the coordinate system $O - xyz$ and the symmetric axis along the z axis illuminated by a plane wave propagating in the xz plane and making an angle, θ_i, with the z axis. The radii of the spheroid in the xy and z directions are a and c, respectively. The two principal curvature radii of the spheroid at $y = 0$ are

$$\rho_1 = \frac{c^2[1 + (a^2/c^2 - 1)z^2/c^2]^{3/2}}{a}, \tag{7}$$

$$\rho_2 = a[1 + (a^2/c^2 - 1)z^2/c^2]^{1/2}. \tag{8}$$

Because of the symmetry of the problem, the wavefront matrix Eq. (5) is simplified to two scalar equations:

$$\frac{k' \cos^2\beta}{R'_1} = \frac{k\cos^2\alpha}{R_1} + \frac{k'\cos\beta - k\cos\alpha}{\rho_1}, \tag{9}$$

$$\frac{k'}{R'_2} = \frac{k}{R_2} + \frac{k'\cos\beta - k\cos\alpha}{\rho_2}, \tag{10}$$

where α and β are respectively the incident and refraction angles. Note that Eqs. (9) and (10) are also valid for reflection by taking $k' = -k$.

Though it is not within the scope of this Letter to discuss diffraction effects, the forward diffraction is simply taken into account by considering the spheroid as an elliptical disk perpendicular to the incident wave. In our case, the two equivalent radii of the ellipse are $A = (c^2 \sin^2\theta_i + a^2\cos^2\theta_i)^{1/2}$ and $B = b$. For the moderate aspect ratio, the amplitude of the forward diffraction wave in far field is given by [10,11]

$$A_d = k^2 Ab \frac{J_1(kA\theta)}{kA\theta},$$

where $\theta = \theta_s - \theta_i$ and θ_s the scattering angle. Notice that if the aspect ratio is important, a more sophisticated model must be used for the diffraction (see [12] and the references therein).

The total field is the contribution of all orders, p, of the complex rays and the forward diffraction. If the particle is absorbent, the attenuation should be considered. By taking into account all these factors, the complex amplitude of a scattered wave in far zone is calculated by

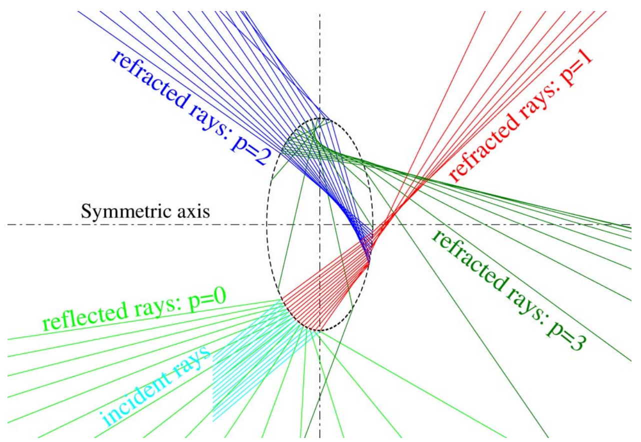

Fig. 1. (Color online) Ray tracing of the first four orders for a spheroid, $a = 2c$, of water ($m = 1.33$) illuminated by a plane wave at 40°. For clarity only a portion of the rays is presented.

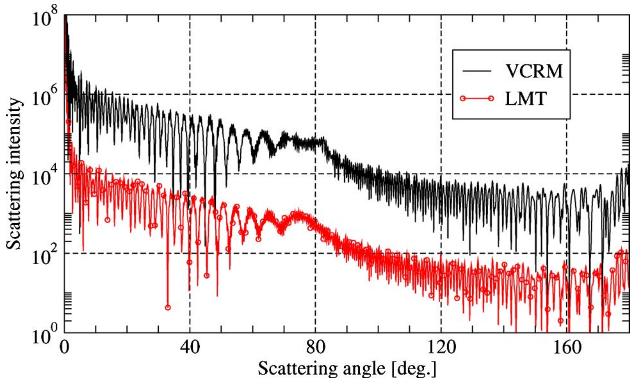

Fig. 2. (Color online) Comparison of scattering diagrams computed by VCRM and LMT for an air bubble in water ($m = 0.75$) of radius $a = 50\ \mu$m illuminated by a plane wave of wavelength $\lambda = 0.6328\ \mu$m. The result of LMT has been offset by a factor of 10^{-2} for clarity.

$$A_\mu = \sum_{p=0}^{\infty} A_{p\mu} e^{-i\Phi_p} e^{-m_i k L_p} + A_d, \qquad (11)$$

where m_i is the imaginary part of the refractive index of the particle, $A_{p\mu}$ the amplitude of the emergent ray of order p with polarization state μ, and L_p the path of the ray in the particle.

Based on the procedure described above, software with a user-friendly interface has been developed under CodeGear Delphi, Borland, USA, and is available by request from the authors. This software makes it possible to visualize the rays of all orders and to calculate the total scattered intensity as well as that of each order for a prolate or oblate spheroid droplet or bubble. As an example, Fig. 1 shows the tracing of rays for a spheroid droplet, $a = 2c$, of water ($m = 1.333$). For clarity, only 15 rays are presented. Rainbows for $p = 2$ and 3 are clearly observed; they are located respectively at 113° and –23°. Some rays are totally reflected within the particle. Of 15 incident rays, seven of $p = 1$ (red) and nine of $p = 3$ (green) exit from the spheroid, and the others are totally reflected.

To validate the calculation of the scattered intensity, we first compare the results of the code with the Lorenz–Mie theory (LMT). Figure 2 shows the scattering diagrams of an air bubble in water illuminated by a vertically polarized plane wave. We find the agreement between VCRM and LMT to be very good. Nevertheless, remarkable difference is found around the critical angle (83°). To improve this, the wave effect must be taken into account.

In the case of a spheroid, the results of VCRM have been compared to that of Lock for the reflection [10] and the first-order refraction [11] in small angles. The agreement is found again to be very good, but our model and software make it possible to predict the scattering diagrams of any orders and in all directions (–180° to 180°). Figure 3 is an example of such diagram. The scattering diagram (calculated with $p_{\max} = 5$) is much more complex than that of a spherical particle. Besides the rainbows seen in Fig. 1 for $p = 2$ and $p = 3$, the rainbows of $p = 4$ at –63° and –106° are more remarkable than those for a sphere.

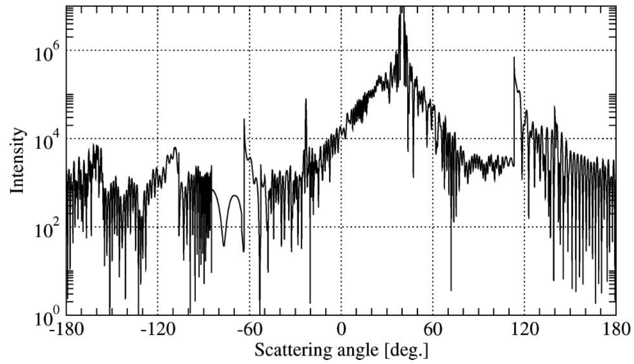

Fig. 3. Scattering diagram of a spheroid ($a = 2c = 20\ \mu$m) of water, $m = 1.333$, illuminated by a plane wave of wavelength $\lambda = 0.6328\ \mu$m at 40°.

The VCRM introduced is suitable for describing the scattering of a smooth surface object of arbitrary shape. By taking into account the interferences of all order complex rays, the VCRM makes it possible to predict the scattering diagrams of a nonspherical particle in all directions. The applications of the model in the 3D scattering of large ellipsoid bubbles [13] and complex liquid ligaments obtained by simulation is under study.

This work was partially supported by the French National Agency under grant ANR-09-BLAN-0023 "CARMINA."

References

1. H. C. van de Hulst, *Light Scattering by Small Particles* (Dover Publications, 1957).
2. A. Macke, M. I. Mishchenko, K. Muinonen, and B. E. Carlson, Opt. Lett. **20** (1995).
3. M. I. Mishchenko, J. W. Hovenier, and L. D. Travis, *Light Scattering by Nonspherical Particles: Theory, Measurements, and Applications* (Academic, 2000).
4. E. A. Hovenac and J. A. Lock, J. Opt. Soc. Am. A **9**, 781 (1992).
5. P. L. Marston, J. Opt. Soc. Am. A **69**, 1205 (1979).
6. P. Yang and K. N. Liou, Appl. Opt. **35**, 6568 (1996).
7. F. Xu, K. F. Ren, and X. Cai, Appl. Opt. **45**, 4990 (2006).
8. F. Xu, K. F. Ren, X. Cai, and J. Shen, Appl. Opt. **45**, 5000 (2006).
9. G. A. Deschamps, Proc. IEEE **60**, 1022 (1972).
10. J. A. Lock, Appl. Opt. **35**, 500 (1996).
11. J. A. Lock, Appl. Opt. **35**, 515 (1996).
12. N. Verrier, S. Coetmellec, M. Brunel, and D. Lebrun, Appl. Opt. **47**, 4147 (2008).
13. F. Onofri, M. Krzysiek, J. Mroczka, K. F. Ren, St. Radev, and J.-P. Bonnet, Exp. Fluids **47**, 721 (2009).